J. Fluid Mech. (1985), *vol.* 154, *pp.* 445–461
Printed in Great Britain

Pressure pulses generated by the interaction of a discrete vortex with an edge

By ARGYRIS G. PANARAS
HAF Technology Research Center (KETA), Palaion Faliron, Athens, Greece

(Received 20 January 1984 and in revised form 10 December 1984)

A central role in the mechanism of the self-sustained oscillations of the flow about cavity-type bodies is played by the reattachment edge. Experimentally it has been found that periodic pressure pulses generated on this edge are fed back to the origin of the shear layer and cause the production of discrete vortices. The oscillations have been found to be suppressed or attenuated when the edge has the shape of a ramp of small angle, or when it is properly rounded. To clarify the role of the shape of the reattachment edge in the mechanism of the oscillations, a mathematical model is developed for the vortex–edge interaction. In this model the interaction of one discrete vortex, imbedded within a constant-speed parallel flow, with the reattachment edge is studied. Two typical shapes of the reattachment edge are examined; a ramp of variable angle and an ellipse. The main conclusion of the present analysis is the strong dependence of the pressure pulses, that are induced on the surface of the edge, on the specific shape of the edge. The pressure pulses on reattachment edges with shapes that give rise to steady flows have been found to be of insignificant amplitude. On the other hand, when the reattachment edge has a shape that is known to result in oscillating flow, the induced pressure pulses are of very large amplitude. Intermediate values of the pressure are found for configurations known to stabilize partially the flow. The present results indicate that, for the establishment of the oscillation, the feedback force generated by the vortex–edge interaction must have an appropriate value. The feedback force may be eliminated if the shape of the lip of the edge is properly designed.

1. Introduction

It is known that the impingement of a shear layer on a boundary may be of an unsteady nature, characterized by the periodic oscillation of the shear layer and the production of discrete sound. Among the diverse configurations that give rise to this unsteady character are the edge tone, the flow past cavities and the impingement of a planar or an axisymmetric jet on a plate. A classification of these flows has been made by Rockwell & Naudascher (1979). They observe that, regardless of the working fluid and flow speed, all of the jet-edge oscillations exhibit qualitatively similar variations of frequency with change in impingement length and flow speed and similar hysteresis effects.

Although the details of the mechanism that induces these self-sustained oscillations are not yet known, it is believed that an essential role is played by the reattachment surface, where periodic pressure disturbances are produced and are fed back to the origin of the inherently unstable free shear layer. There, the pressure disturbances periodically force the shear layer, enhancing its latent coherent structure, so that

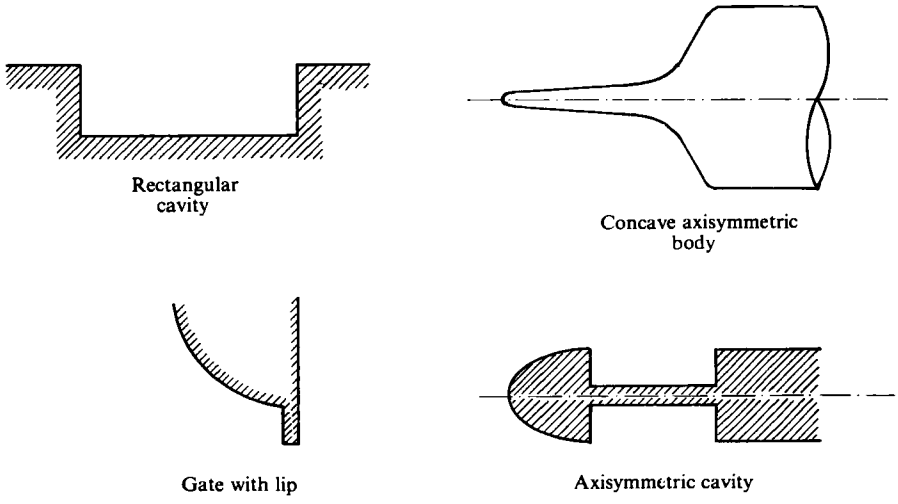

FIGURE 1. Cavity-type bodies.

regular large-scale vortices are produced. The interaction of these vortices with the reattachment surface induces the pressure disturbances.

Early optical detection of the vortical structures of a self-oscillating shear layer was provided by Brown (1937) in his classical smoke-visualization study of the edge-tone, and by Rossiter (1964) who studied the cavity oscillations. More details about the generation of these vortices and their interaction with the reattachment surface were revealed recently, after the work of Brown & Roshko (1974) on the large-scale structure of the turbulent flows and following the development of modern techniques for the detection of coherent structures in shear flows. The work of Rockwell & Knisely (1979), of Ho & Nosseir (1981) and of Ziada & Rockwell (1982) are typical.

Ho & Nosseir (1981), studying a high-speed subsonic jet impinging on a flat plate, were able to detect the two branches of the feedback loop: the downstream convected coherent structures and the upstream propagating pressure waves, which are generated by the impingement of the coherent structures on the plate. Ziada & Rockwell (1982) in their study of the oscillations of an unstable mixing layer impinging upon a wedge have measured the induced force on the wedge by the passing vortices, using a balance and hydrogen-bubble visualization. The interaction of a single vortex, or of patterns of vortices, with a corner has been studied theoretically by Conlisk & Rockwell (1981). They have verified the existence of a pressure pulse induced at the edge as one vortex approaches it.

One basic feature of the feedback mechanism worthy of theoretical study, is the effect of the shape of the reattachment surface on the amplitude of the induced pressure pulses. Such an analysis will be useful in understanding the experimentally observed dependence of the amplitude of oscillation of a shear layer on the shape of the reattachment surface, for the bodies shown in figure 1. Indeed, it has been found that a significant suppression, or even a complete elimination, of the oscillation is possible if the shoulder of the reattachment surface of these cavity-type flows has a shape that does not deflect considerably the impinging shear layer. A brief review of the available experimental data will be presented in §2.

The object of the present work is the aforementioned problem. For the mathematical

modelling the interaction of one line vortex, embedded within a constant-speed parallel flow, with the reattachment surface is examined. The classical method of conformal mapping is applied on two typical shapes of reattachment surface: a ramp of variable angle and an ellipse. The analysis provides the trajectory of the vortex and the corresponding pressure pulses induced on selected points of the edge (reattachment surface).

It will be shown that the amplitude of the pressure pulses depends strongly on the shape of the reattachment surface. More specifically, edges with shapes that result in steady flows, according to the experiments, are characterized by pressure pulses of very low amplitude. On the other hand, the pressure pulses on edges known to induce oscillating flows are of very high amplitude. The remarkable similarity that exists between the influence of an impingement edge and the influence of sound excitation at a discrete frequency, on enhancing the organization of a free shear layer, is used to explain this important conclusion.

2. Suppression of cavity-type oscillations

The term 'cavity-type' used in this work applies to bodies similar to those shown in figure 1. They are characterized by the existence of a planar or an axisymmetric mixing layer, which envelops the separation area formed between the leading and the trailing edge. The possibility of suppressing, or even eliminating, the self-induced oscillations of the shear layer by various techniques is a common characteristic of cavity-type bodies. All the bodies of figure 1 are included in the classification of Rockwell & Naudascher (1979) except for the axisymmetric concave body: however, one of the two modes of instability that have been observed when the high-speed flow about a concave body is unsteady is similar to the classical oscillation of the cavity flows (Panaras 1981). The techniques which have proved successful for the suppression of the oscillation of the flow about a cavity or about a concave body are similar.

In the case of the cavities, the majority of the experimental work concerns appropriate modifications of the geometry of the rectangular cavity. These modifications have been applied to the leading or to the trailing edge of the cavity, or to both. The rounding of the lip or the use of ramps or offsets (figure 2) are the main changes to the trailing edge tested. The tests have been performed in incompressible or supersonic flows. All of these modifications have attenuated, to an extent, the amplitude of oscillations; the use of offsets being the least successful. The most comprehensive studies are those of Ethembambaoglu (1973), Franke & Carr (1975) and Heller & Bliss (1975). Rossiter (1964) has found that installation of leading-edge spoilers is very effective in reducing the magnitude of the pressure fluctuations.

For the case of axisymmetric concave bodies Wood (1962), testing spiked cones at hypersonic Mach numbers, discovered that the separated flow remains steady when the cone angle is smaller than the conical detachment angle. Evidently, this is equivalent to the use of ramps in the cavities. Also, the present author (Panaras 1977) has discovered experimentally at the Von Kármán Institute that a stabilizing parameter of the oscillation mode is the proper rounding of the shoulder of a concave body. The radius of curvature of the shoulder required for the stabilization is scaled to the thickness of the reattaching shear layer. A radius equal to only one-tenth of the diameter of the afterbody proved effective in stabilizing the oscillation about a concave body at a Mach number of 6. Finally, tripping the shear layer by covering the tip of the spike of spiked cylinders with sand or metallic particles proved very effective in suppressing the amplitude of oscillations.

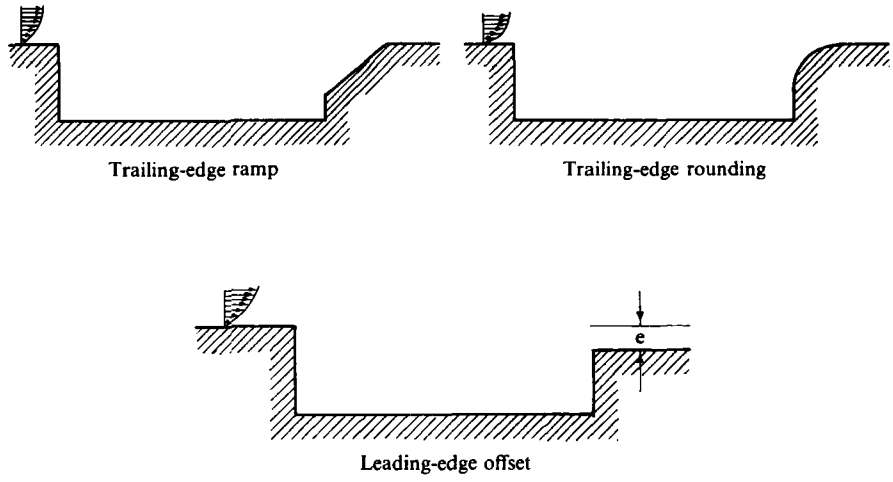

FIGURE 2. Geometrical variations of cavities for attenuation of oscillations.

The problem considered in this paper is closely related to the shear-layer oscillations between the main stream and the plenum chamber of an open jet of a ventilated (slotted or perforated) wind tunnel. Mabey (1971) demonstrated how the shear-layer oscillations could be attenuated, either by covering the slots with flat perforated screens or by rounding the downstream corner of the plenum chamber at the entry to the diffuser.

To conclude, according to the experimental evidence, the self-induced oscillations of the flow about a body similar to one of those shown in figure 1, may be attenuated if:

(*a*) The shoulder of the reattachment edge is rounded or, if sharp, has a small inclination angle or even lies below the leading edge (for cavities).

(*b*) The shear layer is tripped by means of spoilers, sand, etc.

Concerning the role of the tripping, it will be assumed in this paper that, by affecting the state of the otherwise laminar shear layer, the large-scale vortices formed have less energy. Indeed as Roshko (1976) points out, much of the evidence suggests that any important effects of Reynolds number appear indirectly through conditions affecting transition rather than through the direct action of viscosity on the developing turbulent structure. Browand & Latigo (1979), studying the effect of the initial boundary layer upon the downstream growth of the turbulent mixing layer between two streams, concluded that if the mixing layer is tripped by a wire its large-scale structures are relatively suppressed. Kibens (1980) also observed the absence of highly energetic discrete vortices in the shear layer which envelops the potential core of a jet, if the shear layer is turbulent. Finally, Chandrsuda *et al.* (1978) mention that recent experiments strongly suggest that the Brown–Roshko structures will not form if the initial mixing layer is turbulent.

In the next section a simple, incompressible and two-dimensional model will be described for the study of the interaction of a discrete vortex with a reattachment edge. The shape of the edge will be variable. Thus, the effect of the geometrical parameters which, if they are of proper value, stabilize the otherwise oscillating shear layer, will be studied. Considering the existence of a common mechanism that induces the shear-layer oscillation, it is assumed that the results of the present analysis are applicable, qualitatively, to all the cavity-type bodies of figure 1.

3. Description of the model

It is regular practice, in the study of the interaction of one or more vortices with a surface, for the dimensions of the vortices to be ignored. Crighton (1975) reviews the case of the impact of a pair of line vortices of opposite circulation upon a rigid plate and the case of the motion of a line vortex around the edge of a rigid half-plane. The calculated pressure field along the surfaces, in these studies, is used for the estimation of the distant sound field by application of the method of matched asymptotic expansions. The results are similar to those obtained by the Lighthill quadrupole model. The purely hydrodynamic cases of the motion of pairs of line vortices through slits in walls and out of channels, and of the motion of a line vortex over an inclined flat plate, are reviewed by Saffman & Baker (1979). Also, in the vortex–corner interaction of Conlisk & Rockwell (1981), mentioned in the introduction, the assumption of line vortices is made.

Some reservations have been expressed about the simplification of ignoring the finite size of the vortices. The accuracy of the estimated trajectories is questioned. However, Saffman & Baker (1979) state that the centroids of the vortices approach an asymptote monotonically with trajectories qualitatively similar to those of line vortices. Another critical deficiency of this simplification, according to Conlisk & Rockwell (1981), is the inability to accommodate the redistribution of the vorticity and the possible severing of the vortices. However, the same authors note that, according to the experimental data of Rockwell & Knisely (1979), this possible redistribution and severing does not occur until the vortex is very close to, or at, the impingement surface. In addition, the distortion of a vortical structure is limited to a domain which is less than the characteristic vortex diameter upstream of the corner. Furthermore, they mention that details of the vortex distortion at impingement should not substantially influence the trajectories of vortices that are not severed, or clipped, by the corner. Finally, by comparing experimental and calculated vortex trajectories, Conlisk & Rockwell have found that use of a sufficiently weak vortex strength in the line-vortex model allows a reasonable approximation of the trajectories of the laboratory vortices.

The success of the aforementioned studies encourages the application of the line-vortex model in the present case. The method of complex transformations is used. The model is shown in figure 3, in the physical and in the transformed plane. Two special shapes of the edge will be examined, a ramp of variable angle (§3.1) and an ellipse of variable ratio of semi-axes (§3.2).

In the transformed plane the complex velocity potential at a point λ is given by:

$$F(\lambda) = U_\infty \lambda + \mathrm{i}\frac{\Gamma}{2\pi}\ln\frac{\lambda-\lambda_0}{\lambda-\bar{\lambda}_0}, \tag{1}$$

where Γ and λ_0 are respectively the strength and the time-dependent position of the vortex.

In order to obtain the velocity field in the physical plane, knowledge of the transformation $z = f(\lambda)$ is necessary. Then the velocity field is given by the equation:

$$u - \mathrm{i}v = \frac{\mathrm{d}F(\lambda)}{\mathrm{d}\lambda}\frac{1}{f'(\lambda)} = \left[1 + \mathrm{i}\frac{K}{2\pi}\left(\frac{1}{\lambda-\lambda_0} - \frac{1}{\lambda-\bar{\lambda}_0}\right)\right]\frac{1}{f'(\lambda)}, \tag{2}$$

where the velocities have been non-dimensionalized on U_∞, the lengths on edge height b, and $K = \Gamma/U_\infty b$.

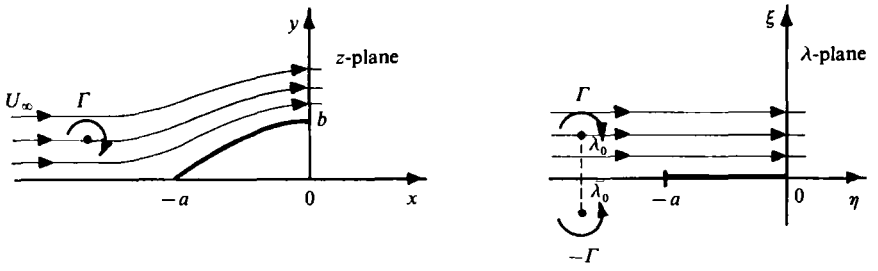

FIGURE 3. The model of the flow.

Equation 2 is valid everywhere except at the vortex position λ_0. For the calculation of the velocity of the vortex, Routh's rule must be used (Clements 1973; Conlisk & Rockwell 1981), leading to:

$$u_0 - iv_0 = \left[1 - i\frac{K}{2\pi(\lambda_0 - \bar{\lambda}_0)}\right]\frac{1}{f'(\lambda_0)} - \frac{iK}{4\pi}\frac{f''(\lambda_0)}{[f'(\lambda_0)]^2}. \tag{3}$$

For the computation of the trajectory of the vortex, from one given initial position upstream of the edge, the following equations will be solved numerically at successive small time steps Δt:

$$\left.\begin{aligned}\frac{dx_0}{dt} &= u_0(x_0, y_0),\\ \frac{dy_0}{dt} &= v_0(x_0, y_0).\end{aligned}\right\} \tag{4}$$

Since the velocity components u_0, v_0 are given in terms of the variable λ_0 and not of z_0 (3), inversion of the transformation $z = f(\lambda)$ is necessary. It will be shown in §3.2 that this inversion is quite simple in the case of the ellipse. However, in the case of the ramp, the transformation is expressed as a hypergeometrical series and the inversion can only be done numerically.

For the purpose of the present study it is necessary to estimate the pressure pulse induced on the edge by a vortex during its movement along its trajectory. An appropriate pressure coefficient that contains only the effect of the vortex and not of the parallel stream is the following one:

$$c_p = \frac{(p_K - p_\infty) - (p - p_\infty)}{q_\infty} = (u^2 + v^2) - (u_K^2 + v_K^2) - \frac{\partial\phi}{\partial t}. \tag{5}$$

Equation (2) is used for the calculation of the velocity components u, v assuming that there is no vortex in the flow ($K = 0$), while the components u_K, v_K include the vortex term ($K \neq 0$). The term $\partial\phi/\partial t$ denotes the non-dimensional unsteady potential.

It is evident from (2) and (5) that the pressure coefficient tends to zero when the vortex is located far upstream of the edge ($|\lambda_0| \gg 1$).

The pressure coefficient will be estimated at some specific points along the edge, so that the distribution of the amplitude of the pressure pulses will be investigated. The points with y-coordinate 0.1, 0.4, 0.6, 0.8, 0.95 have been selected for this purpose and the subscripts $1, 2, \ldots, 5$ have been assigned to these points correspondingly.

For the solution of the equations a PRIME 550/II computer was used, while the graphical presentations of the results were printed in a CALCOMP 1051/907 plotter.

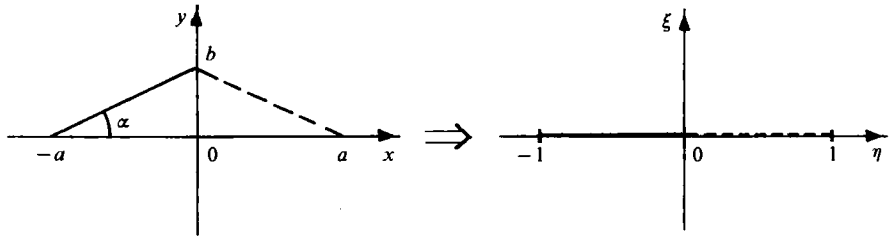

FIGURE 4. Transformation of a ramp.

3.1. *Interaction of a vortex with a ramp*

For the study of the interaction of a vortex with a ramp of angle α (figure 4) the following Schwarz–Christoffel transformation (Spiegel 1964) may be used:

$$z = C\int_0^{\lambda} \frac{g^{2\alpha/\pi}}{(1-g^2)^{\alpha/\pi}}\,\mathrm{d}g + \mathrm{i}b. \tag{6}$$

The value of C can be expressed in terms of the gamma function using the fact that $z = a$ when $\lambda = 1$. It is found that:

$$C = \frac{(a-b\mathrm{i})\,(\pi)^{\frac{1}{2}}}{\Gamma\left(\frac{\alpha}{\pi}+\frac{1}{2}\right)\Gamma\left(1-\frac{\alpha}{\pi}\right)}. \tag{7a}$$

Considering various properties of the gamma function and setting $\delta = \alpha/\pi$, it can be shown that:

$$C = b\,\frac{\Gamma(\frac{1}{2})\,\Gamma(\delta)}{\pi\Gamma(\frac{1}{2}+\delta)}\,\mathrm{e}^{-\mathrm{i}\alpha} = \frac{b}{\pi}\,B(\tfrac{1}{2},\delta)\,\mathrm{e}^{-\mathrm{i}\alpha}. \tag{7b}$$

If $g = \lambda t^{\frac{1}{2}}$ and the z is non-dimensionalized by b, the transformation (6) becomes:

$$z = \frac{B(\frac{1}{2},\delta)}{2\pi}\,\mathrm{e}^{-\mathrm{i}\alpha}\,\lambda^{(1+2\delta)}\int_0^1 t^{(\delta-\frac{1}{2})}\,(1-\lambda^2 t)^{-\delta}\,\mathrm{d}t. \tag{8}$$

For the calculation of this integral the hypergeometric Gauss series included in the tables of Abramowitz & Stegun (1970) are used. This series is defined by the equation:

$$F(d,e;f;h) = \frac{\Gamma(f)}{\Gamma(e)\,\Gamma(f-e)}\int_0^1 t^{e-1}(1-h)^{(f-e-1)}\,(1-ht)^{-d}\,\mathrm{d}t. \tag{9}$$

The hypergeometric series is valid for $\mathrm{Re}\,(f) > \mathrm{Re}\,(h) > 0$ and for all values of h, except for a cut along the real axis from 1 to ∞. Its expression depends on the value of $|h|$:

for $|h| \leqslant 1$:

$$F(d,e;f;h) = 1+\frac{de}{f1!}\,h+\frac{d(d+1)\,e(e+1)}{f(f+1)\,2!}\,h^2+\ldots; \tag{10}$$

for $|h| \geqslant 1$:

$$F(d,e;f;h) = \frac{\Gamma(f)\,\Gamma(e-d)}{\Gamma(e)\,\Gamma(f-d)}\,(-h)^{-d}\,F\left(d,d+1-f;d+1-e;\frac{1}{h}\right) + \frac{\Gamma(f)\,\Gamma(d-e)}{\Gamma(d)\,\Gamma(f-e)}\,(-h)^{-e}\,F\left(e,e+1-f;e+1-d;\frac{1}{h}\right). \tag{11}$$

For the application of the hypergeometric series on the transformation (8) the following equivalence is used:

$$d = \delta, \quad e = \delta + \tfrac{1}{2}, \quad f = \delta + \tfrac{3}{2}, \quad h = \lambda^2.$$

The final result, after several manipulations, is:

for $|\lambda| \leqslant 1$:

$$z = \mathrm{i} + \frac{B(\frac{1}{2}, \delta)}{\pi} \mathrm{e}^{-\mathrm{i}\alpha} \lambda^{(1+2\delta)} \left[\frac{1}{1+2\delta} + \sum_{n=1}^{\infty} \frac{\delta(\delta+1)\dots(\delta+n-1)}{n!\,(2n+1+2\delta)} \lambda^{2n} \right]; \tag{12}$$

for $|\lambda| \geqslant 1$:

$$z = \frac{B(\frac{1}{2}, \delta)}{\pi} \lambda \left[1 - \sum_{n=1}^{\infty} \frac{\delta(\delta+1)\dots(\delta+n-1)}{n!\,(2n-1)} \frac{1}{\lambda^{2n}} \right]. \tag{13}$$

For the numerical calculation of the above series for any value of the angle parameter δ it is sufficient to consider only a few terms. The transformations are very accurate everywhere except at the region of $|\lambda| = 1$. Also, the derivatives are easily estimated. These transformations are developed for the first time in this paper.

If $a \to 0$, $\alpha \to \frac{\pi}{2}$, and (6) is reduced to:

$$z = \mathrm{i} - \mathrm{i} \int_0^{\lambda} \frac{g\,\mathrm{d}g}{(1-g^2)^{\frac{1}{2}}} = (\lambda^2 - 1)^{\frac{1}{2}}. \tag{14}$$

This equation has also been used because of its simplicity.

For the inversion of the transformation, the complex and the real part are separated and then the resulting system of equations is solved numerically by applying the method of Newton described in the algorithm (2.13) of Conte & de Boor (1972). Difficulties in finding the zeros of the system of equations have been experienced at some points near the origin of the axis for $\alpha > 60°$.

A typical example of the application of the present method to the calculation of the interaction of a discrete vortex with a ramp is shown in figure 5. The dashed line denotes the trajectory of the vortex, while the numbered solid lines indicate the value of the pressure coefficient at the correspondingly numbered points of the ramp.

It is observed in figure 5 that, as the vortex approaches the ramp, the induced pressure on its surface increases, initially very slowly, and then it rises rather abruptly when the vortex reaches the vicinity of the ramp. After reaching the maximum value the pressure pulse on each point starts to fall. The amplitude of the pressure pulses is quite small at the base of the ramp, but it becomes very large at its shoulder.

The small discontinuities observed in some curves are due to the shifting of the calculation from one branch of the transformation function (equation 13) to the other (equation 12). This shifting takes place at the point $|\lambda_0| = 1$, where the transformation is not very accurate.

3.2. *Interaction of a vortex with an ellipse*

The ellipse is quite an appropriate geometrical figure for the study of the interaction of a vortex with a curved surface. It is easily transformed into a piece of straight line on the λ-plane by using an intermediate transformation into a circle on the g-plane (figure 6).

The intermediate transformation of the ellipse into the circle, non-dimensionalized by b, is:

$$z = p\left(g + \frac{q}{g}\right), \tag{15}$$

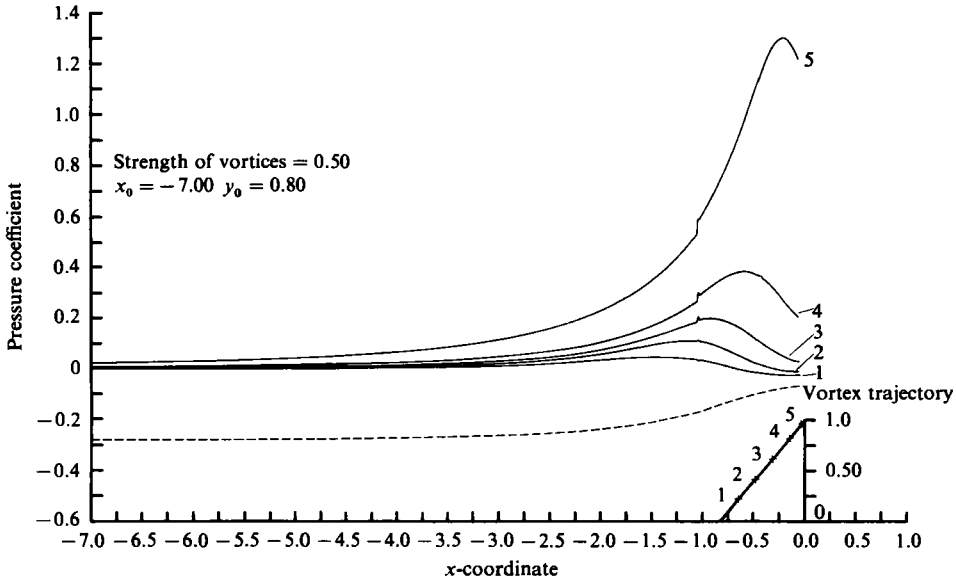

FIGURE 5. Pressure pulses along a ramp of 50°.

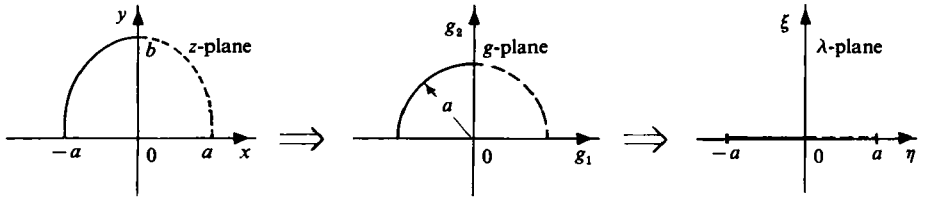

FIGURE 6. Transformation of an ellipse.

where:
$$p = \frac{A+1}{2A}, \quad q = \frac{A-1}{A+1}A^2, \quad A = \frac{a}{b}.$$

The transformation of the circle into the straight line is:

$$\lambda = \frac{1}{2}\left(g + \frac{1}{g}\right). \tag{16}$$

Then the required transformation function $z = f(\lambda)$ and its derivatives are found to be:

$$z = p\left[\lambda + \sqrt{(\lambda^2-1)} + \frac{q}{\lambda + (\lambda^2-1)^{\frac{1}{2}}}\right]; \tag{17}$$

$$f'(\lambda) = \frac{p}{g-\lambda}\,\frac{g^2-q}{g}; \tag{18}$$

$$f''(\lambda) = p\,\frac{(g^2-2g\lambda+q)}{(g-\lambda)^3}. \tag{19}$$

The numerical calculation of a point z_n is easily done in steps, separating the real from the imaginary part, if the corresponding point λ_n, in the λ-plane, is known.

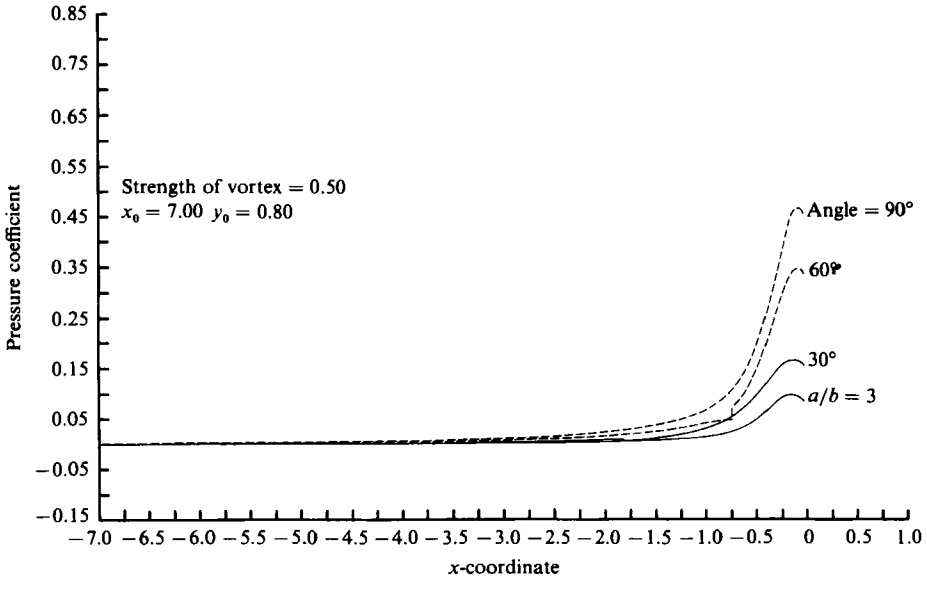

FIGURE 7. The effect on the unsteady potential of the shape of the edge at point 5.

3.3. *Variation of the unsteady potential*

The non-dimensional potential function of the flow model is the real part of (1):

$$\phi = \mathrm{Re}\,(\lambda) + \frac{K}{2\pi}\,[\arg(\lambda - \bar{\lambda}_0) - \arg(\lambda - \lambda_0)]. \tag{20}$$

The temporal variation of this term will be estimated at the points $\lambda_1, \lambda_2, \ldots, \lambda_5$ along the edge, during the motion of a vortex of strength K. Evidently, only the second term contributes to the unsteady potential. It is estimated numerically by using the difference scheme:

$$\left.\frac{\partial \phi}{\partial t}\right|_m = \frac{1}{\Delta t}\,(\phi_{m+1} - \phi_m). \tag{21}$$

More sophisticated schemes would result in higher accuracy. However, the computer-program memory requirements would be increased. For improving the accuracy of the calculations, a variable time step has been applied, with a much smaller value at the vicinity of the edge, where the unsteady potential exhibits significant values, rather than upstream of it.

The variation of the unsteady potential at the point 5 of the edge, for various values of the ramp angle and for an ellipse ($a/b = 3.0$), is shown in figure 7 for $K = 0.5$. It is observed that the unsteady potential always takes positive values, i.e. it tends to reduce the pressure induced on the edge by the passing vortex, see (5). Also its maximum value depends strongly on the shape of the edge. Besides, it has been found that near the base of the edge the unsteady potential takes very small values.

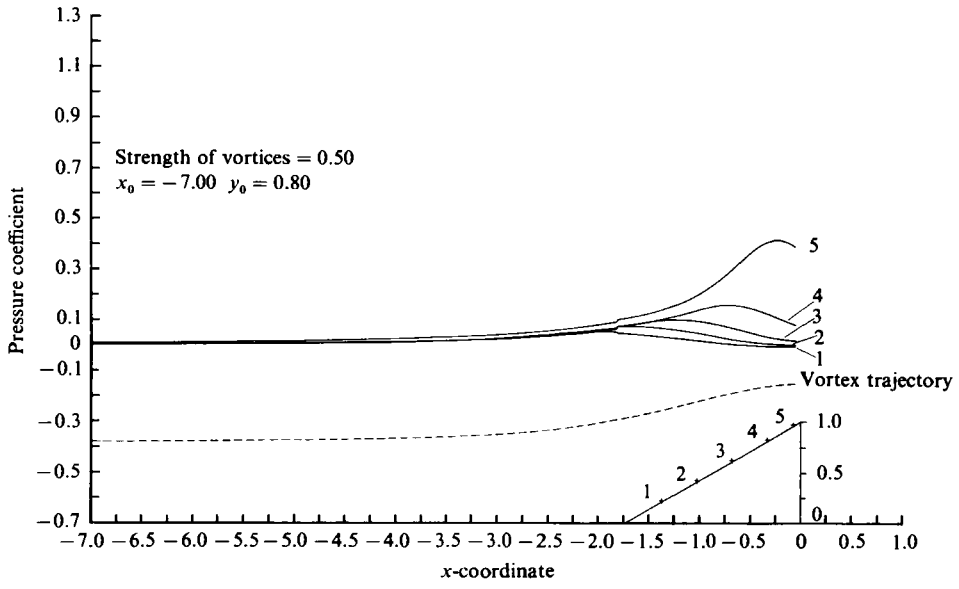

FIGURE 8. Pressure pulses along a ramp of 30°.

4. Application of the method

The various parameters that have been found experimentally to affect the behaviour of the flow about a cavity-type body will be examined in this section, by using the mathematical model described previously. These parameters are: the shape of the reattachment edge; the initial y-coordinate; and the strength of the vortex.

According to Conlisk & Rockwell (1981) the range of the non-dimensional strength of vortices generated in cavity flows in laboratory experiments is $K = 0.1$–0.6. These values will be used in the present work.

4.1. *Effect of the shape of the edge*

The optimization of the shape of the reattachment edge has been found to be the most effective means of suppressing the self-excited oscillations. A ramp of small angle is a very efficient shape in this sense. In figures 8 and 9 the trajectories of a vortex of strength $K = 0.5$ and the induced pressure fields along ramps of 30° and 90° angles, respectively, are shown.

When comparing figures 5, 8 and 9 one may see that, if the ramp angle increases, the trajectory of the vortex approaches the edge and the induced pressure pulses at the shoulder increase abruptly. Thus, for $\alpha = 90°$ the amplitude of the pressure pulse at point 5 of the ramp is almost an order of magnitude higher than the amplitude at the equivalent point of a ramp with $\alpha = 30°$. It is noted here that, according to the experimental evidence, the flow about cavities equipped with reattachment ramps of $\alpha = 30°$ is steady, while the flow about regular rectangular cavities oscillates.

In all cases shown in the aforementioned figures, the amplitude of the pressure pulses is significant only at the edge of the ramp, while it has low values at its base. This feature suggests that for the suppression of the self-excited oscillations of the flows about the bodies shown in figure 1, it is sufficient to optimize only the lip of the reattachment surface and not its base. This rule has already been empirically applied in various experimental studies.

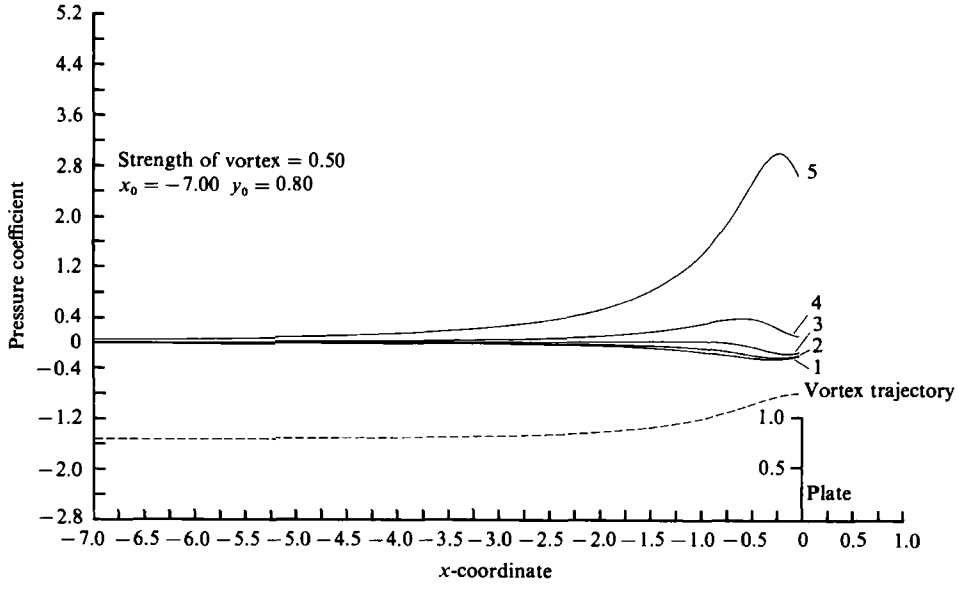

FIGURE 9. Pressure pulses along a ramp of 90°.

The small value of the width of the pressure pulses at the lip of the edge is another remarkable feature of the pressure field (figures 5, 9). For example it is seen in figure 9 that, if the vortex lies upstream of the edge at a distance equal to its height ($x = -1.0$), the induced pressure is reduced to half of its maximum value. If the vortex lies further upstream, at $x = -2.0$, its contribution to the pressure pulses is only one-sixth of the maximum value. Thus, the contribution of a vortex to the induced pressure field at the edge is reduced very abruptly when its distance from the edge is increased. If a row of vortices is considered, it seems then that a small spacing or wavelength λ is required for the production of discrete pulses. In this case the mean value of the pulses will be greater, because of the contribution of the other vortices.

For the definition of the minimum wavelength above which pressure pulses are generated, the combined effect of all the vortices of the row must be considered. However, from the dynamics of the interaction of one vortex (figures 5, 9) the approximate value $m = \lambda/b < 1$ may be assumed. Besides, according to Ziada & Rockwell (1982), the length of a cavity is connected to the wavelength by the relation $L = \lambda n$, where n is an integer. Thus the following useful equation is derived:

$$\frac{L}{b} = nm. \tag{22}$$

This equation states that the critical length of a cavity for the onset of oscillations ($n = 1$), and for the appearance of higher modes ($n = 2, 3, \ldots$), depends linearly on the appropriate value which the spacing of the generated vortices should have so that discrete pulses will be induced at the reattachment edge. The definition of the appropriate value of the parameter m and its dependence on the initial conditions of the flow are outside the scope of this work and of the capability of the computer program used.

The proper rounding of the reattachment edge is another successful means of suppressing the self-excited oscillations of cavity-type flows.

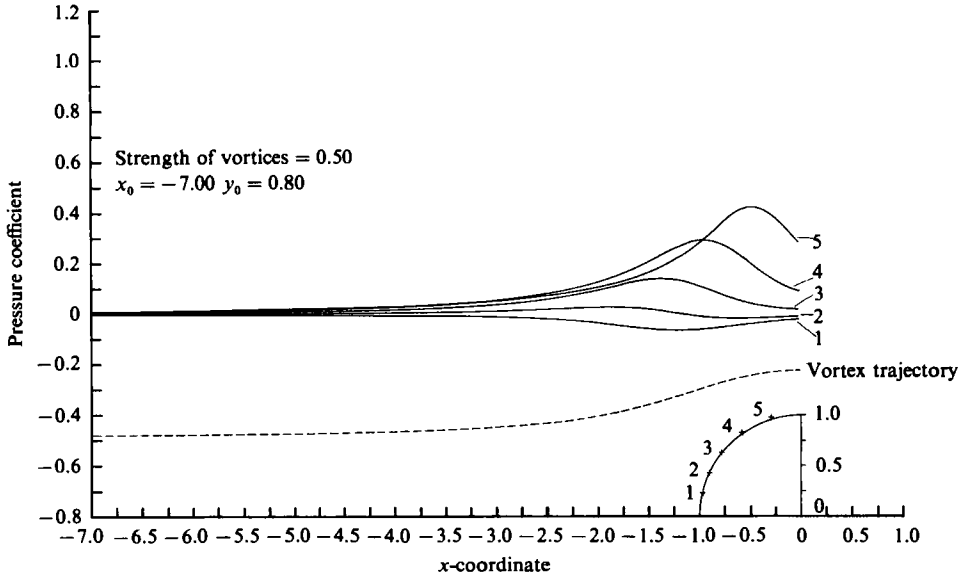

FIGURE 10. Pressure pulses along a circle.

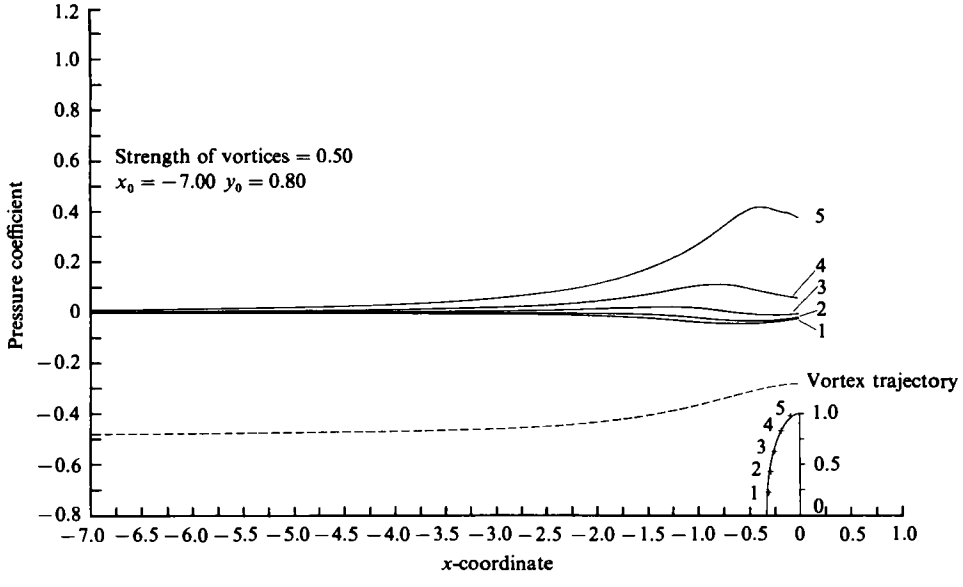

FIGURE 11. Pressure pulses along an ellipse, ratio of ellipse axes = 3.0.

For the study of the effect of a curved edge on the amplitude of the induced pressure pulses, two cases of vortex–ellipse interactions are shown in figures 10, 11 for ratio of ellipse axis equal to 1.0 and 3.0. In both cases the strength of the vortex is $K = 0.5$. It is noted that the flow about all these ellipses should be non-oscillating, which is because the non-dimensional radius of curvature at their edges is somewhat greater than the value $\frac{1}{10}$, which has been experimentally found to result in steady flows (see §2).

It is remarkable that, though in these figures a rather broad range of curvature

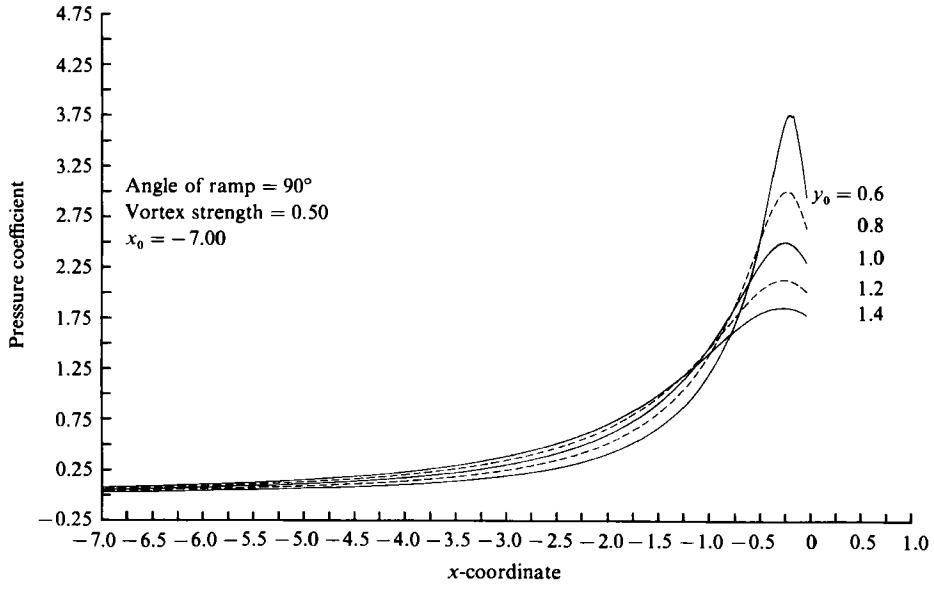

FIGURE 12. The effect of the initial vertical distance of the vortex from the edge on the amplitude of the pressure pulses, for ramps of $\alpha = 90°$.

of the lip of the reattachment surface is represented, nevertheless the amplitude of all the pressure pulses is very small compared to the ones of the rectangular cavity (figure 9). Their maximum value is about equal to the one observed on the ramp of $\alpha = 30°$.

4.2. *Effect of geometrical offsets*

The lowering of the trailing edge of a rectangular cavity is one technique effective to some degree in attenuating the shear-layer oscillations, though not so successful as the use of ramps or the rounding of the edge. Ethembabaoglu's (1973) experimental data lead to an estimation of a 30% reduction of the cavity pressure fluctuations for a 20% offset of the leading edge.

For studying this effect here, the initial vertical distance of the vortex is used as a parameter. The results of such a calculation are shown in figure 12. It is observed that the amplitude of the pressure pulses depends strongly on this parameter. More specifically, if the vortex initially lies below the lip of the edge ($y_0 < 1.0$) the pressure amplitude is greater than when it lies above the lip ($y_0 > 1$). It is noted in figure 12 that the rate of change of the amplitude of the pressure is higher for values of $y_0 < 1$.

The curves of figure 12 indicate that the forcing mechanism has small intensity when, according to the experimental evidence, the amplitude of the oscillations is small. It is also seen that, in the case of the rectangular cavity, the level of the forcing function does not reach the low values observed in the oscillation-free case of the ramp of 30°, even if the offset distance of its leading edge takes very high values ($y_0 = 1.4$).

However, it is evident that, if the trailing edge has the shape of a ramp, the application of offset may have a more profound effect on the suppression of the oscillations.

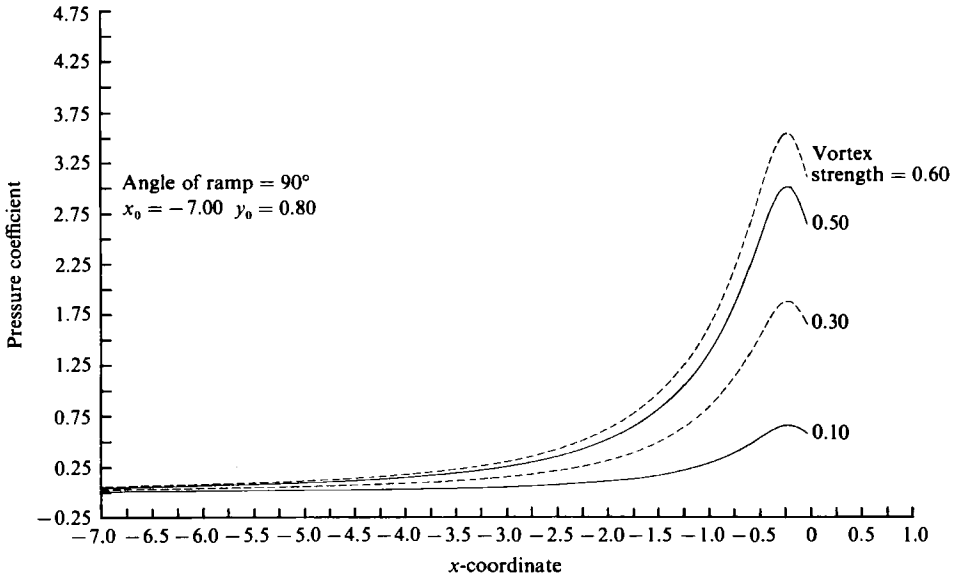

FIGURE 13. The effect of the strength of the vortices on the amplitude of the pressure pulses, for ramps of $a = 90°$.

4.3. *Effect of the strength of the vortices*

The strength of the interacting vortices is a basic parameter of the present model. Its effect on the induced-pressure pulses is shown in figure 13 for the case of the vertical plate ($\alpha = 90°$). It is observed that, if the strength of the vortices is small ($K = 0.10$), the pressure pulses have the same order of magnitude as those induced on an oscillation-free configuration (a small-angle ramp or an ellipse) but with vortices of much higher strength.

As has already been mentioned in §2, it may be assumed that small values of the strength of the discrete vortices may simulate the existence of spoilers in an appropriate position of a rectangular cavity or of a concave axisymmetric body. These mechanisms have proven quite effective in reducing the oscillations. The results of figure 13 seem to enforce the hypothesis concerning the role which the spoilers play in the reduction of the oscillations. Still, comprehensive laboratory measurements are required to validate this evidence.

5. Discussion and conclusions

The strong dependence of the pressure pulses, that are generated by the vortex–edge interaction, on the specific shape of the edge is the main conclusion of the present analysis. More specifically, it has been found that the induced pressure pulses on ramps of small angle or ellipses have very small amplitude, even for large values of the strength of the interacting vortices. On the other hand, the pressure amplitude on steep ramps is very large.

Also, it has been shown experimentally that the flow about the cavity-type bodies shown in figure 1 is steady when their trailing edge has the shape of a ramp of small angle or when it is rounded, while the flow is oscillating when the ramp angle is large.

The above comparison indicates that, for the establishment of sustained oscillations

in a cavity, the existence of a periodic feedback force of certain value is necessary. To explain this, recourse to the experimental evidence is required. To our knowledge no one has studied experimentally the effect of the geometry of the reattachment edge of a cavity on the development of the structure of the shear layer.

However, detailed studies have been performed on the influence of sound excitation of variable amplitude, at a discrete frequency, on enhancing the organization of a free-shear layer. Experimental evidence seems to support the view that similarity exists between these types of flow. This similarity was discovered by Rockwell & Knisely (1979) when they compared the velocity spectra with and without insertion of the reattachment edge of a cavity, to those measured by Miksad (1972) in a non-impinging shear layer with and without application of sound at a discrete frequency.

Clear evidence of the role of the level of acoustic forcing in the development of a laminar low-speed shear layer has been provided by Freymuth (1966). He has discovered that, the lower the level of forcing, the longer is the length of the shear layer required for the growth of the instabilities to the saturation limit and, consequently, for the appearance of organized vortices.

A similar conclusion was reached very recently by Gharib (1983). One of the objectives of his investigation was to study the receptivity of a cavity shear layer to externally imposed disturbances, for a cavity length less than the one required for the onset of self-sustained oscillations. His flow-visualization pictures showed that, while in the oscillation mode periodic vortices are produced near the reattachment edge, in the case of the steady flow no vortices are observed. Gharib applied variable forcing at various frequencies. Spectral analysis of the response-velocity fluctuations indicated that the level of shear-layer response at all the frequencies increased with the forcing power. But, when the forcing reached a threshold level, resonance appeared at the forcing frequency in which the shear-layer satisfies the phase criterion ($L = \lambda n$). When he increased the length of the cavity, Gharib observed that the resonance peak appeared at a lower forcing level, an indication that the threshold level decreases as the length of the cavity increases.

Gharib (1983) concludes that it is logical to propose that, as the cavity length increases, the threshold level decreases to such an extent that a flow background frequency, which satisfies the phase criterion and has sufficient amplitude, will initiate the self-sustained oscillation.

It is concluded then that, in view of the present analysis, it seems that the oscillations are initiated and sustained by the periodic pressure pulses induced by the vortex–edge interaction, provided that the geometry of the edge is such that the amplitude of the pressure pulses is sufficient.

We hope that the present analysis has introduced new evidence for the role of the vortex–edge interaction in the mechanism of the self-sustained oscillations of cavity-type flows, and that it will stimulate further experimental research in appropriate laboratories. It could also prove useful for the design of cavity-type configurations free of oscillations.

The author would like to thank Dipl. Eng. D. Kazandzis, former student at the University of Patras, for his assistance in the evaluation of integral (8). Thanks are also due to Mr E. Alexandridis (M.Sc.) of KETA for his pertinent advice on using the PRIME 550 computer and to Dr X. Aslanoglou for his assistance in preparing the graphics.

REFERENCES

ABRAMOWITZ, M. & STEGUN, I. A. 1970 *Handbook of Mathematical Functions*. New York: Dover.

BROWAND, F. K. & LATIGO, B. O. 1979 Growth of the two-dimensional mixing layer from a turbulent and non-turbulent boundary layer. *Phys. Fluids* **22**, 1011–1019.

BROWN, G. B. 1937 The vortex motion causing edge tones. *Proc. Phys. Soc.* **49**, 493–507.

BROWN, G. L. & ROSHKO, A. 1974 On density effects and large structures in turbulent mixing layers. *J. Fluid Mech.* **64**, 775–816.

CHANDRSUDA, C., MEHTA, R. D., WEIR, A. D. & BRADSHAW, P. 1978 Effect of free-stream turbulence on large structure in turbulent mixing layers. *J. Fluid Mech.* **85**, 693–704.

CLEMENTS, R. R. 1973 An inviscid model of two-dimensional vortex shedding. *J. Fluid Mech.* **57**, 321–336.

CONLISK, A. T. & ROCKWELL, D. 1981 Modeling of vortex–corner interaction using point vortices. *Phys. Fluids* **24**, 2133–2142.

CONTE, S. D. & DE BOUR, C. 1972 *Elementary Numerical Analysis. An Algorithmic Approach*. McGraw-Hill.

CRIGHTON, D. G. 1975 Basic principles of aerodynamic noise generation. *Prog. Aero. Sci.* **16**, 31–96.

ETHEMBABAOGLU, S. 1973 On the fluctuating flow characteristics in the vicinity of gate slots. *Division of Hydraulic Engineering, University of Trondheim, Norway.*

FRANKE, M. E. & CARR, D. L. 1975 Effect of geometry on open cavity flow-induced pressure oscillations. *AIAA paper* 75-492, *AIAA 2nd Aero-Acoustics Conf., Hampton, Va., March 24–26.*

FREYMUTH, P. 1966 On transition in a separated laminar boundary layer. *J. Fluid Mech.* **25**, 683–704.

GHARIB, M. 1983 The effect of flow oscillations on cavity drag, and a technique for their control. Ph.D. thesis, California Institute of Technology.

HELLER, H. H. & BLISS, D. 1975 The physical mechanism of flow-induced pressure fluctuations in cavities and concepts for their suppression. *AIAA Paper* 75-491, *AIAA 2nd Aero-Acoustics Conf., Hampton, Va., March 24–26.*

HO, C. M. & NOSSEIR, N. S. 1981 Dynamics of an impinging jet. Part 1. The feedback phenomenon. *J. Fluid Mech.* **105**, 119–142.

KIBENS, V. 1980 Discrete noise spectrum generated by an acoustically excited jet. *AIAA J.* **18**, 434–441.

MABEY, D. G. 1971 Flow unsteadiness and model vibrations in wind tunnels at subsonic and transonic speeds. *ARC CP* 1155.

MIKSAD, R. W. 1972 Experiments on the nonlinear stages of free-shear transition. *J. Fluid Mech.* **56**, 695–719.

PANARAS, A. G. 1977 Design criteria for the non-occurrence of high speed unsteady separation about concave bodies. *AGARD Conf. Proc.* 227, *paper* 30.

PANARAS, A. G. 1981 Pulsating flows about axisymmetric concave bodies. *AIAA J.* **19**, 804–806.

ROCKWELL, D. & KNISELY, G. 1979 The organized nature of flow impingement upon a corner. *J. Fluid Mech.* **93**, 413–432.

ROCKWELL, D. & NAUDASCHER, F. 1979 Self-sustained oscillations of impinging free shear layers. *Ann. Rev. Fluid Mech.* **11**, 67–94.

ROSHKO, A. 1976 Structure of turbulent shear flows: a new look. *AIAA J.* **14**, 1349–1357.

ROSSITER, J. E. 1964 Wind tunnel experiments on the flow over rectangular cavities at subsonic and transonic speeds. *RAE Rep. and Memoranda No.* 3438.

SAFFMAN, R. G. & BAKER, G. R. 1979 Vortex interactions. *Ann. Rev. Fluid Mech.* **11**, 95–122.

SPIEGEL, M. R. 1964 *Complex Variables*. Schaum's Outline Series. McGraw-Hill.

WOOD, C. 1962 Hypersonic flow over spiked cones. *J. Fluid Mech.* **12**, 614–624.

ZIADA, S. & ROCKWELL, D. 1982 Oscillations of an unstable mixing layer impinging upon an edge. *J. Fluid Mech.* **124**, 307–334.